

LOW-GWP REFRIGERANTS: PERFORMANCE ASSESSMENT AND SELECTION TRADEOFFS

**Piotr A. Domanski^(a), Riccardo Brignoli^(a),
J. Steven Brown^(b), Andrei F. Kazakov^(c), Mark O. McLinden^(c)**

- (a) Energy and Environment Division, National Institute of Standards and Technology
Gaithersburg, MD 20899, USA, piotr.domanski@nist.gov
(b) Department of Mechanical Engineering, The Catholic University of America
Washington, DC 20064, USA, brownjs@cua.edu
(c) Applied Chemicals and Materials Division, National Institute of Standards and Technology
Boulder, CO 80395, USA, andrei.kazakov@nist.gov

ABSTRACT

The merits of an alternative refrigerant are established based on many attributes including environmental acceptance, chemical stability in the refrigeration system, low toxicity, flammability, efficiency and volumetric capacity. In an earlier work, these criteria were used to screen a comprehensive database to search for refrigerants with low global warming potentials (GWP). The present paper summarizes the screening process and presents the performance of the ‘best’ 27 replacement fluids for small and medium-sized air-conditioning, heating, and refrigeration applications. In addition to considering cycle calculations based only on thermodynamic properties, a simulation model that included transport properties and optimized heat exchangers was used to assess the performance potentials of the candidate fluids. The need for this more detailed modeling approach is demonstrated for systems relying on forced-convection evaporation and condensation. The study shows that the low-GWP refrigerant options are very limited, particularly for fluids with volumetric capacities similar to those of R-410A or R-404A. The probability of finding ‘ideal’, better-performing low-GWP fluids is minimal.

Keywords: Air Conditioning, COP, Global Warming Potential, Refrigerants, Volumetric Capacity

1. INTRODUCTION

As anticipated for some time, an addendum to the Montreal Protocol adopted in October 2016 requires a significant reduction of the weighted value of global warming potential (GWP) of fluids used in air-conditioning and refrigerant equipment (UNEP, 2016). Consequently, hydrofluorocarbon (HFC) refrigerants having a high GWP will be eliminated or their use will be significantly reduced. Hence, new replacement fluids with a low GWP must be found. This paper presents results of our multiyear study, in which we searched for low-GWP replacement refrigerants for small and medium-sized air-conditioning (AC), heat pumping, and refrigeration equipment. Such systems are comprised of a positive-displacement compressor, air-to-refrigerant condenser and evaporator, expansion device, and associated fans and controls. R-410A (a blend of the HFCs R-32 and R-125) is the dominant refrigerant in this equipment category, with the exception of commercial refrigeration applications where R-404A (a blend of the HFCs R-32, R-143a, and R-134a) is very common. R-22, a hydrochlorofluorocarbon refrigerant (HCFC), was most commonly used prior to the introduction of HFCs, and is still used in developing countries.

Our search for low-GWP replacement fluids relied on the screening of a comprehensive database of chemical substances. To this database we applied filters representing different refrigerant selection criteria to reject unsuitable molecules and reduce the pool of candidates to only plausible fluids. This reduced pool of fluids underwent two rounds of thermodynamic cycle simulations, which revealed the group of the ‘best’ 27 low-GWP refrigerants.

In the course of this comprehensive project we published several papers to communicate intermediate results. Among them, Domanski et al. (2014) discussed the performance limits of the vapor compression cycle, McLinden et al. (2014) reported results of the first database screening and described refrigerant selection

tradeoffs, and McLinden et al. (2015) presented the results of the improved second database screening and provided cycle performance information based on simplified simulations for AC applications. The most complete description of the project is given in McLinden et al. (2017), which provides the final list of the ‘best’ 27 fluids with the cooling mode performance from cycle simulations with optimized heat exchangers, and includes a complete description of the screening methodology with an extensive list of references.

The current paper summarizes the second (final) screening of the database, discusses the importance of refrigerant thermophysical properties and heat exchanger optimization in cycle simulations, and provides a combined presentation of the performance of the ‘best’ 27 fluids in air conditioning [originally reported in McLinden et al. (2017)], heating, and refrigeration applications.

2. DATABASE SCREENING

The merits of a candidate replacement fluid are established based on many attributes including GWP (low value desired), ozone depletion criteria (ODP, zero or very low), chemical stability in the refrigeration system, toxicity (low value desired), flammability (low value desired), and cycle performance parameters, i.e., COP and volumetric capacity (Q_{vol}). Practical attributes include compatibility with the system materials, although this consideration is typically considered in the later phase of the refrigerant selection process.

To search for the most suitable low-GWP refrigerants, we used the PubChem database listing over 60 million unique chemical molecules (Kim, et al., 2016). The concept of our study relied on establishing filters representing different refrigerant selection criteria and applying them to the molecules listed in PubChem. We accepted the thermodynamic argument that viable refrigerants are restricted to small molecules (McLinden, 1990), and we considered PubChem to be exhaustive for such molecules.

The effectiveness of database screening processes depends on the quality of established filters and the sequence in which they are applied. The results of the first screening (McLinden et al., 2014) provided us insights, based on which we changed the sequence of screens for a second screening. For this second (final) database screening, we limited our search to molecules with 18 or fewer atoms and comprising only the elements C, H, F, Cl, Br, O, N, or S, following the observation by Midgley (1937) that only a small portion of the periodic table would form compounds volatile enough to serve as refrigerants. Also excluded were ions, radicals, and molecules enriched in specific isotopes. Despite their ability to deplete stratospheric ozone, we included Cl and Br since molecules comprising Cl or Br might have a negligible ODP and might be acceptable if they have a very short atmospheric lifetime. These restrictions reduced the pool of molecules for further consideration to 184 000.

The next two screens involved GWP_{100} and T_{crit} . The PubChem database does not provide these data for the vast majority of the compounds, so they had to be estimated using novel methods developed within this study (Kazakov et al., 2012, Carande et al., 2014, Carande et al., 2016); the development and application of these estimation methods constituted a major effort of the study. These methods were based solely on the molecular structure. The prediction of GWP_{100} combined estimates of the radiative efficiency and atmospheric reactivity with the hydroxyl radical. The tradeoff of computational efficiency versus accuracy was a major consideration given the large number of compounds to screen. The method achieved a logarithmic root mean square deviation of 3.0 for the GWP_{100} estimate compared to available literature values, and this accuracy was considered adequate for screening purposes. The estimates of critical temperature were done using the method presented in Kazakov et al., (2010).

The applied screens of $GWP_{100} < 1000$ and $320 \text{ K} < T_{crit} < 420 \text{ K}$ reduced the pool of candidates to 138 fluids, as listed in McLinden et al. (2017). The limits on T_{crit} were based on experience with refrigerants used in small AC systems, with an allowance for the uncertainty in the T_{crit} estimation method. The limit of 1000 for GWP_{100} also provided an allowance for the estimation uncertainty and considered that, for example, refrigerants with $GWP_{100} < 750$ are permitted under EU regulations in AC systems with refrigerant charge under 3 kg (EU, 2014).

The next screens were for chemical stability and toxicity; both were applied manually. Compounds with generally unstable functional groups were dropped from further consideration. These included peroxides (compounds with the $-O-O-$ group), ketenes (compounds with the $-C=C=O$ group), and allenes (compounds

with the $-C=C=C-$ group). Compounds with a carbon-carbon triple bond were generally dropped as less stable than those with a double bond; for example, fluoroethyne ($FC\equiv CH$) is described as “treacherously explosive in the liquid state.” (Middleton et al., 1959). There were exceptions, however, and trifluoropropyne was retained.

For the toxicity screen, in addition to considering functional groups, e.g., $=CF_2$ and $-OF$, the analysis involved a manual examination of toxicity data from a variety of sources, such as safety standards, material safety data sheets (MSDS), compilations of toxic industrial chemicals, and regulatory filings. McLinden et al. (2017) provide more detailed discussion.

In this second (final) screening, we did not apply the flammability filter but rather used flammability as an attribute to be considered as a tradeoff in the final refrigerant selection. We opted for this approach following a review of results of the first screening (McLinden et al., 2014) in which a flammability filter rejected a large number of flammable fluids, some of which perhaps could be used in several applications after implementing appropriate hazard mitigation measures.

3. PERFORMANCE EVALUATION

Performance merits of refrigerants are defined by COP and Q_{vol} obtained at specified operating conditions. There is an inherent tradeoff between COP and Q_{vol} , which can be related to the refrigerant critical temperature; fluids with a high T_{crit} tend to have a high COP and low Q_{vol} , and vice versa (Domanski et al., 2014). In this sense, the applied screen $320\text{ K} < T_{crit} < 420\text{ K}$ ensured that the accepted 138 low-GWP fluids had the COP and Q_{vol} in a general range of those of currently used refrigerants. The imposed T_{crit} range corresponded to air-conditioning applications, and we carried out a further refrigerant selection process using operating conditions representative of air conditioning (AHRI, 2008). Accurate estimations of COP and Q_{vol} of candidate fluids required thermodynamic cycle simulations. To manage the level of effort of the selection process, we performed two rounds of simulations at different levels of detail. Our final simulations included the basic thermodynamic cycle, cycle with a liquid-line/suction line heat exchanger (LL/SL-HX), and two-stage economizer cycle (Figure 1).

3.1 First round cycle simulations

In the first round, we simulated the performance of candidate fluids in an air-conditioning application in the basic thermodynamic cycle (Figure 1(a)), as implemented in the CYCLE_D model (Brown et al., 2015), with an imposed evaporating temperature of $10\text{ }^\circ\text{C}$ and condensing temperature of $40\text{ }^\circ\text{C}$, and with the ideal assumptions of zero pressure drop in the heat exchangers and a 100 % efficient compression process. To better elucidate thermodynamic trends, we performed these simulations on the complete list of 138 low-GWP candidates (i.e., including the unstable or toxic fluids), and also included an additional eight currently used refrigerants. For the representation of refrigerant properties, we used the detailed equations of state (EOS) implemented in the NIST REFPROP database (Lemmon et al., 2013), where available. However, for a majority of the fluids we used the extended corresponding states (ECS) model (McLinden et al., 2012).

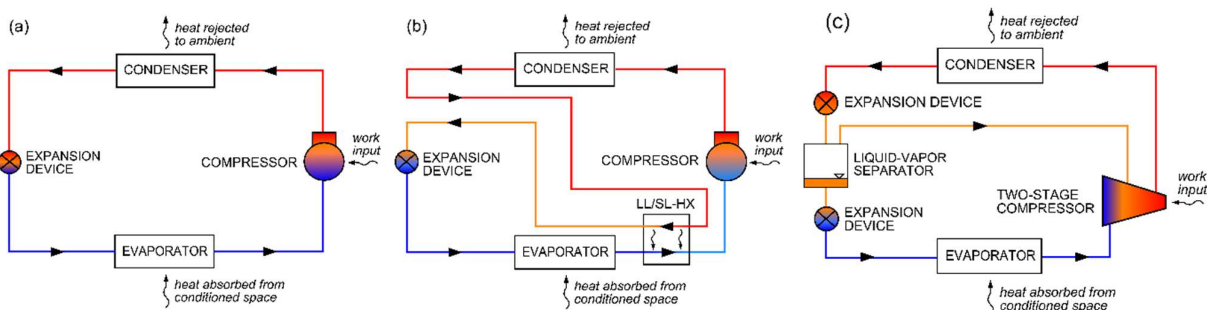


Figure 1: Schematic of (a) basic cycle, (b) cycle with liquid-line/suction line heat exchanger (LL/SL-HX), and (c) two-stage economizer cycle

Figure 2 presents COPs and volumetric capacities obtained from the first round simulations. The figure clearly shows the COP versus Q_{vol} tradeoff, which results from an ideal analysis based only on thermodynamic properties (McLinden, 1988). The figure also includes a Pareto Front, which represents the COP limit for

‘ideal’ hypothetical fluids allowed by thermodynamics (Domanski et al., 2014). At this stage, we dropped fluids with a volumetric capacity less than one-third that of R-410A or a COP < 5. (For R-410A in the ideal cycle $Q_{vol} = 6.62 \text{ MJ}\cdot\text{m}^{-3}$ and COP = 7.41. The volumetric capacity of R-22 is 66 % that of R-410A, so this would correspond to dropping fluids with a capacity less than one-half that of R-22.) This yielded a set of less than 30 low-GWP fluids for simulations in greater detail in the second simulation round.

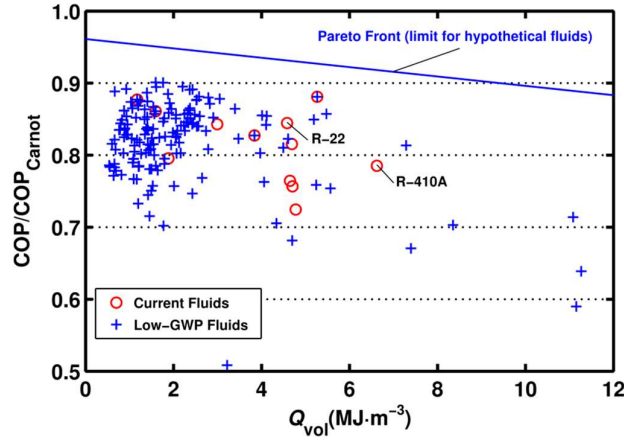


Figure 2: Ratio of COP to the Carnot COP in the ideal basic cycle for air-conditioning (McLinden et al., 2015)

3.2 Second round cycle simulations

The second round of simulations used a more advanced cycle model, which is referred to as CYCLE_D-HX (Brignoli et al., 2017). The CYCLE_D-HX model builds on the concept of using temperature profiles of the heat sink and heat source, and the mean effective temperature differences between the refrigerant and heat transfer fluids (ΔT_{hx}) in the evaporator and condenser (Domanski and McLinden, 1992). This modeling approach facilitates accounting for refrigerant thermophysical properties, pressure drop, and heat-transfer coefficient on the cycle performance on a relative basis (Brown et al., 2002a and 2002b). Most importantly, it provides a more realistic representation of an air conditioner employing typical forced-convection, air-to-refrigerant heat exchangers, which are optimized for a particular refrigerant. In this type of heat exchanger, the refrigerant undergoes a phase change as it flows down the inside of a tube and exchanges heat with air on the outside of the tube. CYCLE_D-HX accounts for the effect of optimized refrigerant mass flux, which enhances the refrigerant heat transfer coefficient at an acceptable penalty of pressure drop, as described by Brown et al. (2002b).

To examine the importance of the optimization of refrigerant circuitry, consider that a pressure drop in the evaporator or condenser causes a saturation temperature drop and results in increased mean effective temperature differences ΔT_{hx} in the heat exchangers. The refrigerant heat-transfer coefficient h also affects ΔT_{hx} ; a higher h yields a lower ΔT_{hx} . A decrease in condenser and evaporator ΔT_{hx} lowers the temperature lift seen by the compressor and subsequently lowers the compressor work, which improves the COP. The heat-transfer coefficient h and pressure drop Δp are both a function of the refrigerant mass flux G , where h approximately increases proportionally to $G^{0.8}$, while Δp increases proportionally to G^2 (Collier and Thome, 1994). There is an optimum value of G that provides a best compromise between the opposite effects that h and Δp have on the system COP.

Figure 3 shows the dependency of h and Δp on the mass flux in evaporation at $T_{sat} = 0 \text{ }^\circ\text{C}$ for R-32, R-1234yf, and R-717 (ammonia). We used correlations by Wojtan et al. (2005a and 2005b) and Muller-Steinhagen and Heck (1986) for generating data for h and Δp , respectively. The results shown are normalized by nominal h and Δp values for R-32 at $G_{nom} = 100 \text{ kg}\cdot\text{m}^{-2}\cdot\text{s}^{-1}$, $h_{nom} = 3.16 \text{ kW}\cdot\text{m}^{-2}\cdot\text{K}^{-1}$ and $\Delta p_{nom} = 1.26 \text{ kPa}$, respectively. All values are average values calculated by Eq. (1):

$$F = \frac{1}{x_{End} - x_{Start}} \int_{x_{Start}}^{x_{End}} f(x), \quad (1)$$

where $f(x)$ is h or Δp , x_{start} is the quality corresponding to the isenthalpic expansion from a condenser saturation temperature of $45 \text{ }^\circ\text{C}$ and 3 K subcooling to evaporator conditions of $T_{sat} = 0 \text{ }^\circ\text{C}$, and $x_{End} = 1$.

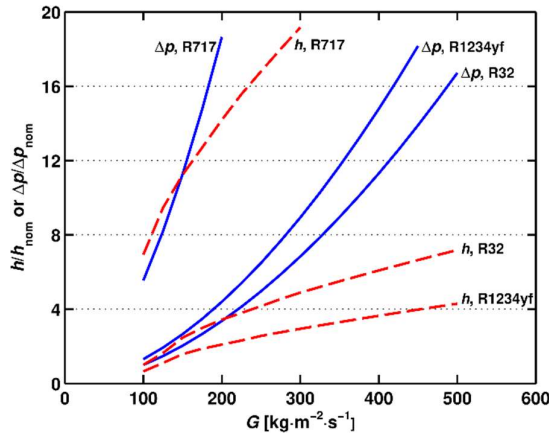


Figure 3: Effect of refrigerant mass flux on forced-convection evaporation and pressure drop

Figure 3 shows that an increase in refrigerant mass flux causes exponential increases in the pressure drop but only asymptotically increases the heat-transfer coefficient. First, comparing R-32 (a high-pressure fluid) and R-1234yf (a medium-pressure fluid), R-1234yf has a lower heat-transfer coefficient and a higher pressure drop than R-32 at the same mass flux, and the rate of increase of heat-transfer coefficient in relation to pressure drop is less favorable for R-1234yf than for R-32. Also, the drop of saturation temperature of R-1234yf is greater than that of R-32 for the same pressure drop. For example, at $T_{\text{sat}} = 0\text{ }^{\circ}\text{C}$, $dT/dp = 0.0934\text{ K}\cdot\text{kPa}^{-1}$ for R-1234yf and $dT/dp = 0.0384\text{ K}\cdot\text{kPa}^{-1}$ for R-32, which leads to a 2.4 times greater decrease in saturation temperature for R-1234yf than for R-32 at the same pressure drop. Similar trends take place in condensing flows.

The optimum refrigerant mass flux G is different for each refrigerant and depends on refrigerant thermodynamic and transport properties. Ammonia, for example, which has a very high thermal conductivity and moderate saturation temperature drop due to its low vapor density, will realize the best compromise between heat-transfer coefficient and pressure drop at a low mass flux, i.e., at a high number of parallel tube circuits. On the other hand, R-32, being a higher-pressure fluid (higher vapor density) and having lower liquid thermal conductivity than ammonia, will realize the best compromise between heat transfer and pressure drop penalization at a higher mass flux, i.e., at a lower number of circuits.

Among other modeling considerations, CYCLE_D-HX maintained the same heat flux in the evaporator through all simulations, which is a prerequisite for a fair rating of competing refrigerants (Domanski and McLinden, 1992). The isentropic efficiency of the compressor was at about the 70 % level, and it differed between the fluids as it was a function of refrigerant thermodynamic properties (Brignoli et al., 2017). The more detailed cycle analysis implemented in CYCLE_D-HX yielded fluid COP and Q_{vol} that are different from those obtained from CYCLE_D simulations based on thermodynamic properties alone (Figure 4a and 4b). The CYCLE_D results show refrigerants with a low Q_{vol} having a higher COP than high-capacity fluids. This COP-versus-capacity tradeoff is not maintained in the CYCLE_D-HX results; the maximum COP corresponds to Q_{vol} of approximately 60 % to 110 % of that of R-410A.

It is important to understand the disparity in the COP-versus-capacity trends between CYCLE_D and CYCLE_D-HX simulations. With the same (imposed) saturation temperatures in the evaporator and condenser, CYCLE_D-type simulations tend to yield higher COPs for low-pressure refrigerants compared to high-pressure refrigerants because low-pressure fluids operate far below their critical point and tend to exhibit less irreversibilities due to the superheated vapor horn and throttling process (Domanski and Didion, 1993). However, this thermodynamic advantage of low-pressure fluids can be erased in systems using heat exchangers that implement refrigerant forced-convection evaporation and condensation (e.g., air-to-refrigerant coils) because low-pressure fluids have low vapor density and therefore exhibit relatively large pressure and saturation temperature drops in forced-convection coils. These irreversibilities may render high-pressure refrigerants more efficient, particularly when refrigerant circuitries (and therefore mass fluxes) in these heat exchangers are optimized, which was done in the CYCLE_D-HX simulations.

subclass 2L) using the color yellow, and denote class 3 fluids with red. Current air-conditioning systems predominantly use class 1 (non-flammable) refrigerants; switching to flammable refrigerants requires the examination of involved risks and the development of safety measures. A significant amount of research in this area has been undertaken by industry already and is still ongoing. We may note that the only non-flammable low-GWP refrigerant in the figures, R-1225ye(Z), has a capacity only of about 25 % of R-410A and a substantially lower COP. It has a low acute toxicity (Lindley and Noakes, 2010) but showed toxic effects for longer exposures at 500 $\mu\text{L/L}$ – 1000 $\mu\text{L/L}$ (500 ppm – 1000 ppm by volume in air) (Schuster, 2009).

Table 1. COP and volumetric capacity of selected low-GWP fluids and current HFC and HCFC fluids in the basic and two-stage economizer (Econ.) cycles. Values are from CYCLE_D-HX simulations with optimized heat exchangers relative to the performance in the basic cycle of R-410A and R-404A for heating and refrigeration, respectively. GWP₁₀₀ are estimated by the method of Kazakov et al., (2010) unless noted. The fluids are grouped by chemical class and, within classes, listed in order of increasing critical temperature.

IUPAC Name	Structure	ASHRAE Designation	GWP ₁₀₀	Heating				Refrigeration			
				COP		$\frac{Q_{vol}}{Q_{vol,R-410A}}$		COP		$\frac{Q_{vol}}{Q_{vol,R-404A}}$	
				Basic	Econ.	Basic	Econ.	Basic	Econ.	Basic	Econ.
Hydrocarbons and dimethylether											
Ethane	CH ₃ -CH ₃	R-170	6†	§		§		§		§	
Propene (propylene)	CH ₂ =CH-CH ₃	R-1270	2†	1.025	1.051	0.703	0.797	1.119	1.189	1.055	1.281
Propane	CH ₃ -CH ₂ -CH ₃	R-290	3†	1.004	1.039	0.572	0.651	1.082	1.167	0.841	1.028
Methoxymethane (dimethylether)	CH ₃ -O-CH ₃	R-E170	1†	0.960	1.010	0.360	0.394	0.944	1.083	0.482	0.565
Cyclopropane	-CH ₂ -CH ₂ -CH ₂ -	R-C270	86	0.994	1.025	0.456	0.500	1.027	1.123	0.645	0.756
Fluorinated alkanes (HFCs)											
Fluoromethane	CH ₃ F	R-41	116†	§		§		§		§	
Difluoromethane	CH ₂ F ₂	R-32	677†	1.025	1.042	1.077	1.193	1.096	1.162	1.601	1.892
Fluoroethane	CH ₂ F-CH ₃	R-161	4†	1.000	1.034	0.576	0.636	1.049	1.142	0.824	0.972
1,1-Difluoroethane	CHF ₂ -CH ₃	R-152a	138†	0.939	0.994	0.360	0.392	0.907	1.059	0.474	0.553
1,1,2,2-Tetrafluoroethane	CHF ₂ -CHF ₂	R-134	1120†	0.911	0.989	0.304	0.333	0.830	1.034	0.378	0.447
Fluorinated alkenes (HFOs) and alkynes											
Fluoroethene	CHF=CH ₂	R-1141	<1†	1.002	1.031	1.440	1.666	1.083	1.158	2.169	2.707
1,1,2-Trifluoroethene	CF ₂ =CHF	R-1123	3	0.984	1.029	1.105	1.302	1.055	1.160	1.623	2.087
3,3,3-Trifluoroprop-1-yne	CF ₃ -C≡CH	n.a.	1.4	0.968	1.023	0.520	0.593	1.003	1.139	0.724	0.902
2,3,3,3-Tetrafluoroprop-1-ene	CH ₂ =CF-CF ₃	R-1234yf	<1†	0.934	1.003	0.391	0.452	0.940	1.104	0.527	0.672
(E)-1,2-Difluoroethene	CHF=CHF	R-1132(E)	1	0.987	1.025	0.557	0.613	1.022	1.127	0.784	0.922
3,3,3-Trifluoroprop-1-ene	CH ₂ =CH-CF ₃	R-1243zf	<1†	0.938	0.997	0.346	0.388	0.942	1.084	0.468	0.566
1,2-Difluoroprop-1-ene‡	CHF=CF-CH ₃	R-1252ye‡	2	0.935	0.995	0.323	0.359	0.917	1.066	0.428	0.509
(E)-1,3,3,3-tetrafluoroprop-1-ene	CHF=CH-CF ₃	R-1234ze(E)	<1†	0.892	0.974	0.283	0.317	0.841	1.034	0.360	0.439
(Z)-1,2,3,3,3-pentafluoro-1-propene	CHF=CF-CF ₃	R-1225ye(Z)	<1†	0.884	0.963	0.246	0.279	0.843	1.022	0.315	0.391
1-Fluoroprop-1-ene‡	CHF=CH-CH ₃	R-1261ze‡	1	0.931	0.991	0.361	0.342	0.879	1.046	0.406	0.474
Fluorinated oxogenates											
Trifluoro(methoxy)methane	CF ₃ -O-CH ₃	R-E143a	523†	0.922	0.991	0.333	0.374	0.905	1.067	0.440	0.536
2,2,4,5-Tetrafluoro-1,3-dioxole	-O-CF ₂ -O-CF=CF-	n.a.	1	0.881	0.967	0.292	0.326	0.810	1.017	0.365	0.439
Fluorinated nitrogen and sulfur compounds											
N,N,1,1-tetrafluoromethanecamine	CHF ₂ -NF ₂	n.a.	20	0.975	1.028	0.817	0.962	1.034	1.155	1.174	1.510
Difluoromethanethiol	CHF ₂ -SH	n.a.	1	0.980	1.024	0.544	0.601	1.010	1.129	0.761	0.903
Trifluoromethanethiol	CF ₃ -SH	n.a.	1	0.947	1.002	0.388	0.431	0.956	1.094	0.526	0.630
Inorganic compounds											
Carbon dioxide	CO ₂	R-744	1.00†	§		§		§		§	
Ammonia	NH ₃	R-717	<1†	0.990	1.022	0.665	0.706	0.954	1.081	0.898	1.022
Current HFCs and HCFC											
Pentafluoroethane	CF ₃ -CHF ₂	R-125	3170†	0.937	1.007	0.757	0.914	0.971	1.126	1.056	1.423
R-32/125 (50.0/50.0)	blend	R-410A	1924	1.000	1.040	1.000	1.145	1.000	1.143	1.000	1.306
Chlorodifluoromethane	CHClF ₂	R-22	1760†	0.998	1.028	0.653	0.724	1.053	1.144	0.941	1.119
1,1,1,2-Tetrafluoroethane	CF ₃ -CH ₂ F	R-134a	1300†	0.930	0.998	0.391	0.437	0.913	1.081	0.518	0.627

*Values are relative to those for R-410A or R-404A in the basic cycle:

COP_{R-410A} = 4.68 and $Q_{vol,R-410A}$ = 4.85 MJ·m⁻³; COP_{R-404A} = 2.68 and $Q_{vol,R-404A}$ = 1.85 MJ·m⁻³

†Literature value from Myhre et al., (2013) or E.U. regulation (EU, 2014)

‡This fluid has cis (Z) and trans (E) isomers; the predicted values of both were the same.

§Fluid would be near-critical or supercritical in the condenser and was not simulated.

4.1 Air conditioning

The reference operating conditions for the R-410A air conditioner corresponded to an evaporating temperature of 10 °C and a condensing temperature of 40 °C. The discussion presented here follows McLinden et al., (2017) where these results were first reported, including Figures 4(b), 5(a), 5(b) and the list of the ‘best’ 27 fluids with numerical values for COP and Q_{vol} . From Figure 4(b) which presents results for the basic cycle, the maximum COP corresponds to Q_{vol} of approximately 60 % to 110 % of that of R-410A, however, a significant agglomeration of fluids occurs for Q_{vol} smaller than 60 %. These are the lower-pressure fluids on the list. They tend to achieve low COPs in systems with forced-convection evaporators and condensers (Figure 4(b)), although they would have a performance advantage in systems with shell-and-tube heat exchangers (Figure 4(a)). The COP of the basic vapor compression cycle ranges from -7.8 % to +5.5 % relative to that of R-410A (13.3 % range). Ammonia shows the highest COP, better than that for R-410A by 5.5 %. Beyond ammonia, which is toxic, mildly flammable, and presents materials compatibility issues, the COPs of R-32, propene (R-270), R-161, R-1132(E), propane (R-290), cyclopropane (R-C270) and difluoromethanethiol are also above the R-410A baseline. The COPs of the remaining fluids are lower. Mildly flammable R-32 has a COP and Q_{vol} higher than that of R-410A, but this advantage comes with a GWP₁₀₀ of 677. R-134 and R-E143a have GWP₁₀₀ values of 1120 and 523, respectively. Three fluids have GWPs within the 80 to 150 range, and GWPs for the remaining fluids do not exceed 20. Except for R-32, R-1123, and R-1141, the listed fluids have Q_{vol} lower than R-410A and would thus require a larger compressor — by at least 25 % and, for a majority of the candidates, more than twice as large—to provide the same capacity as R-410A.

The list of 27 fluids includes six novel molecules: tetrafluorodioxole, trifluoromethanethiol, trifluoropropyne, difluoromethanethiol, (E)-1,2-difluoroethene (R-1132(E)), and tetrafluoromethanamine. Little data are available on these fluids so their risks are unknown, but their performance does not stand out and does not provide a compelling reason for a substantial research effort. Difluoromethanethiol and (E)-1,2-difluoroethene, for example, have predicted COPs slightly higher than R-410A, but Q_{vol} values that are about 40 % lower than that of R-410A. They are flammable (in addition to possible other hazards), and their COP and Q_{vol} are very similar to propane (R-290). It does not seem reasonable to take on the unknown risks of these fluids when one could use the somewhat more flammable, but well-known propane.

In addition to the basic cycle, the cooling mode simulations included a cycle with a LL/SL-HX and a two-stage economizer cycle. These two advanced cycles can be used to improve a refrigerant’s performance by minimizing throttling irreversibilities. Figure 5(a) presents COP and Q_{vol} of the selected fluids in a cycle with a LL/SL-HX. The results are given with a reference to the R-410A values for the basic cycle. The addition of the LL/SL-HX to the cycle benefits fluids with a large molar heat capacity but may degrade the performance of fluids with a small molar capacity (Domanski, 1995). For example, the COP of R-410A improved with respect to the COP in the basic cycle by 1.2 %. A significant improvement (up to 5.4 %) of COP is noted for most HFOs, which are larger molecules and tend to have larger molar heat capacities. On the other hand, ammonia and R-32 (best performers in the basic cycle), which are small molecules with smaller molar heat capacities, achieved lower COPs in the LL/SL-HX cycle than in the basic cycle. Since the LL/SL-HX penalized best performers and improved the worst performers, the range of observed COPs is reduced to 8.1 % for the LL/SL-HX cycle, from 13.3 % for the basic cycle.

The application of the two-stage economizer cycle improves performance of all fluids, with the fluids performing worse in the basic cycle achieving a greater improvement than the best performers. Here, R-410A improved by 4.9 %, the COP of R-32 and ammonia is about 3.2 % and 2.5 % better than in the basic cycle, but others e.g., R-1234ze(E) improved by over 6 %. Except for R-1225ye(Z) and tetrafluorodioxole, the COP of each fluid in the economizer cycle exceeded the COP of R-410A in the basic cycle, but only six fluids had a higher COP if compared to the that of R-410A in the same economizer cycle.

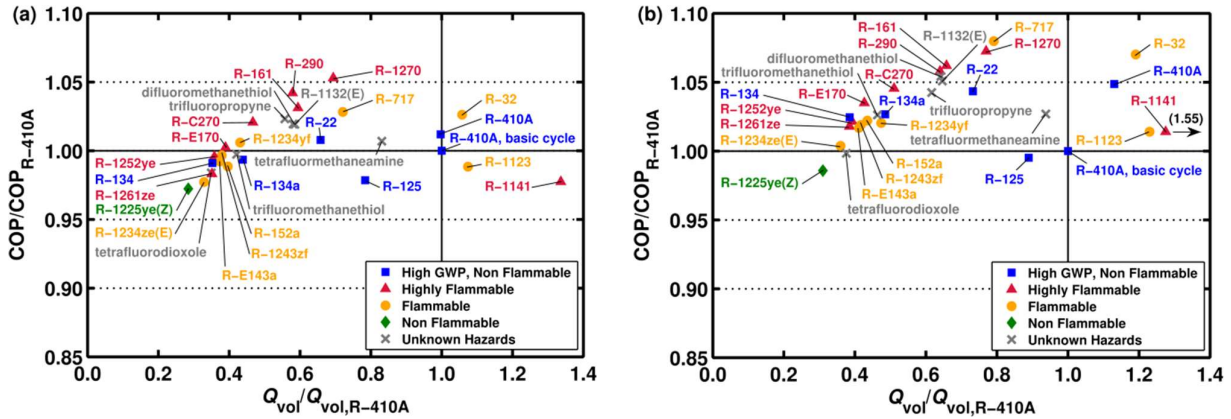


Figure 5: COP and Q_{vol} of selected fluids referenced to R-410A values; (a) cycle with LL/SL-HX, and (b) two-stage economizer cycle; CYCLE_D-HX simulations for an air-conditioning application

4.2 Heating

We simulated the selected fluids for the heating application with reference to a heat pump using R-410A. The reference operating conditions corresponded to an evaporating temperature of $-10\text{ }^{\circ}\text{C}$ and a condensing temperature of $30\text{ }^{\circ}\text{C}$. The general pattern for the heating operation is similar to the pattern we discussed for the cooling operation. I.e., the agglomeration of low-GWP fluids occurs for low values of Q_{vol} , and the fluids with low values of Q_{vol} have low COPs. One difference may be noted that COPs of refrigerants with a low Q_{vol} (Figure 6(a)) are a few percentage points lower with respect to R-410A than those for the cooling operation (Figure 4(b)). Two reasons can be given for this observation:

(1) The lower evaporation temperature during heating operation ($-10\text{ }^{\circ}\text{C}$ for heating vs. $10\text{ }^{\circ}\text{C}$ for cooling) results in lower refrigerant density in the evaporator for the heating operation, which effects a larger refrigerant pressure drop and saturation temperature drop during the heating mode; the low-pressure (low- Q_{vol}) fluids are more sensitive to this penalty.

(2) The lower condensing temperature in heating operation ($30\text{ }^{\circ}\text{C}$ for heating vs. $40\text{ }^{\circ}\text{C}$ for cooling) moves the high-pressure side of the thermodynamic cycle away from the refrigerant's critical temperature, and this move is of more benefit for the high-pressure (high- Q_{vol}) fluids, such as R-410A.

The above statement applies to a comparison of heating versus cooling in the economizer cycles as well (Figures 5(b) and 6(b)).

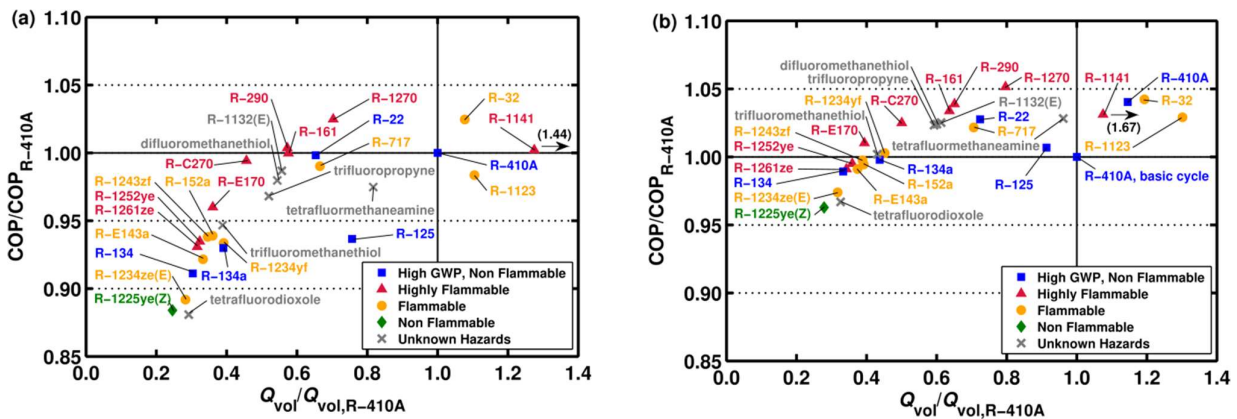


Figure 6: COP and Q_{vol} of selected fluids referenced to R-410A values from CYCLE_D-HX simulations for a heating application; (a) basic cycle, and (b) two-stage economizer cycle

4.3 Refrigeration

We simulated the selected fluids for the refrigeration application with the reference to a system using R-404A (Figure 7). The reference operating conditions corresponded to an evaporating temperature of $-20\text{ }^{\circ}\text{C}$ and a condensing temperature of $30\text{ }^{\circ}\text{C}$. The general pattern for the refrigeration operation is similar to the pattern we discussed for the cooling and heating cycles. Specifically, the low-pressure (low- Q_{vol}) refrigerants have substantially lower COPs in the basic cycle than does R-404A. The COP spread between the low- Q_{vol} and high- Q_{vol} is over 30 %, the largest of the three operating conditions simulated. For the economizer cycle, the COP spread is reduced to 17.2 %, although this is still substantial. R-1270 showed the best COP, the same result as for the heating operation.

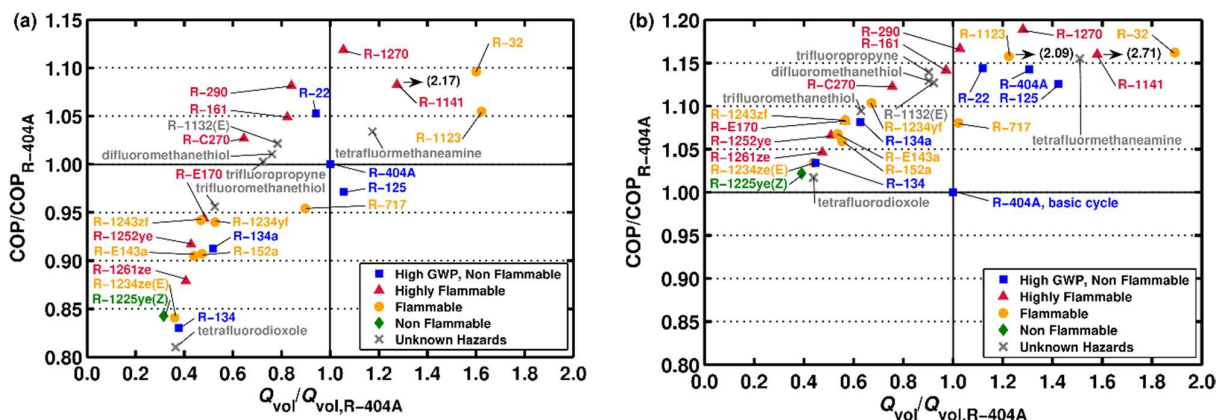


Figure 7: COP and Q_{vol} of selected fluids referenced to R-404A values from CYCLE_D-HX simulations for a refrigeration application; (a) basic cycle and (b) two-stage economizer cycle

CONCLUSIONS

Our search for single-component low-GWP fluids for use in small air-conditioning, heating, and refrigeration systems showed that the refrigerant options for these applications are very limited, particularly for fluids with volumetric capacities similar to R-410A or R-404A. The identified fluids with good COP and low toxicity are at least mildly flammable. Refrigerant blends can be used to increase flexibility in choosing tradeoffs between COP, volumetric capacity, flammability, and GWP.

Accepting the thermodynamic argument that viable refrigerants are restricted to small molecules, it is our contention that our screening process yielded a list of the ‘best’ low-GWP fluids, i.e., the probability of finding any better-performing low-GWP single-component fluid subject to the criteria and constraints applied at this particular historical moment is minimal.

Most of the identified fluids are relatively large molecules with relatively large molar heat capacities. As such, these fluids experience greater throttling losses in the basic vapor-compression cycle than currently used HFC refrigerants and will benefit from implementation of the LL/SL-HX cycle or economizer cycle, which can minimize throttling irreversibilities.

Performance of different refrigerants in systems employing heat exchangers relying on forced-convection evaporation and condensation heat transfer do not exhibit a tradeoff between COP and volumetric capacity observed for an ideal cycle analysis based on thermodynamic properties alone. Refrigerant screening for such systems needs to include transport properties and heat exchanger optimization.

ACKNOWLEDGEMENT

This work was supported by the U.S. Department of Energy, Office of Energy Efficiency and Renewable Energy under contract no. DE-EE002057 with A. Bouza and B. Habibzadeh serving as Project Managers.

NOMENCLATURE

AC	air conditioning	LL/SL-HX	liquid-line/suction-line heat exchangers
COP	coefficient of performance	MSDS	material safety data sheet
G	mass flux ($\text{kg}\cdot\text{m}^{-2}\cdot\text{s}^{-1}$)	ODP	ozone depletion potential
GWP	global warming potential	p	pressure (kPa)
GWP ₁₀₀	GWP for a time horizon of 100 years	Q_{vol}	volumetric capacity ($\text{kJ}\cdot\text{m}^{-3}$)
HCFC	hydrochlorofluorocarbon	T	temperature (K or °C)
HFC	hydrofluorocarbon	x	refrigerant quality (fraction)
HFO	hydrofluoroolefin		
h	enthalpy ($\text{kW}\cdot\text{m}^{-2}\cdot\text{K}^{-1}$)		

Subscripts and symbols

crit	critical	sat	saturation
hx	heat exchanger	Δ	difference
nom	nominal		

REFERENCES

- AHRI, 2008. ANSI/AHRI Standard 210/240-2008 for Performance Rating of Unitary Air-Conditioning & Air-Source Heat Pump Equipment. Air-Conditioning, Heating, and Refrigeration Institute, Arlington, VA.
- ASHRAE, 2013. ANSI/ASHRAE Standard 34-2013 Designation and Safety Classification of Refrigerants. ASHRAE, Atlanta, GA.
- Brignoli, R., Brown, J.S., Skye, H., Domanski, P.A., 2017. Refrigerant Performance Evaluation Including Effects of Transport Properties and Optimized Heat Exchangers, in preparation.
- Brown, J.S., Kim, Y., Domanski, P.A., 2002a. Evaluation of Carbon Dioxide as R22 Substitute for Residential Conditioning, ASHRAE Transactions, 108(2), 954-963.
- Brown, J.S., Yana-Motta, S.F., Domanski, P.A., 2002b. Comparative analysis of an automotive air conditioning system operating with CO₂ and R134a, Int. J. Refrig., 25(1), 19-32.
- Brown, J.S., Domanski, P.A., Lemmon, E.W., 2015. NIST Standard Reference Database 49, CYCLE_D: NIST Vapor Compression Cycle Design Program, version 5.0. (Standard Reference Data Program, National Institute of Standards and Technology, Gaithersburg, MD, 2012).
- Carande, W. H.; Kazakov, A.; Muzny, C.; Frenkel, M., 2014. Quantitative structure-property relationship predictions of critical properties and acentric factors for pure compounds. J. Chem. Engr. Data 60, 1377-1387.
- Carande, W., Kazakov, A., Kroenlein, K., 2016. Comparison of machine learning algorithms for the prediction of critical values and acentric factors for pure compounds. In 251st ACS National Meeting, San Diego, March 13-17, 2016; CINF 163.
- Collier, J.G., Thome, J.R., 1994. Convective Boiling and Condensation. Clarendon Press, Oxford.
- Domanski, P.A., 1995. Minimizing Throttling Losses in the Refrigeration Cycle, Proceedings of the 19th Int. Congress of Refrig., The Hague, The Netherlands, August 21-25, 1995, Int. Inst. Refrig., Paris, France., 766-773.
- Domanski, P.A., McLinden, M.O., 1992. A Simplified Cycle Simulation Model for the Performance Rating of Refrigerants and Refrigerant Mixtures, Int. J. Refrig., 15(2), 81-88.
- Domanski, P.A., Didion, D.A., 1993. Thermodynamic Evaluation of R-22 Alternative Refrigerants and Refrigerant Mixtures, ASHRAE Transactions, 99(2), 636-648.
- Domanski, P.A., Yashar, D., 2006. Comparable Performance Evaluation of HC and HFC Refrigerants in an Optimized System, 7th IIR Gustav Lorentzen Conference on Natural Working Fluids, Trondheim, Norway.
- Domanski, P. A., Brown, J. S., Heo, J., Wojtusiak, J., McLinden, M. O., 2014. A thermodynamic analysis of refrigerants: Performance limits of the vapor compression cycle. Int. J. Refrig. 38, 71-79, doi:10.1016/j.ijrefrig.2013.09.036

- EU, 2014. European Parliament. Regulation (EU) No 517/2014 of the European Parliament and of the Council of 16 April 2014 on fluorinated greenhouse gases and repealing Regulation (EC) No 842/2006
- Kazakov, A., Muzny, C. D., Diky, V., Chirico, R. D., Frenkel, M., 2010. Predictive correlations based on large experimental datasets: Critical constants for pure compounds. *Fluid Phase Equilib.* 298, 131-142.
- Kazakov, A., McLinden, M. O., Frenkel, M., 2012. Computational design of new refrigerant fluids based on environmental, safety, and thermodynamic characteristics. *Ind. Eng. Chem. Res.* 51, 12537-12548, doi:10.1021/ie3016126
- Kim, S. et al., 2016. PubChem substance and compound databases. *Nucleic Acids Res.* 44, D1202-D1213, doi:10.1093/nar/gkv951
- Lemmon, E.W., Huber, M.L., McLinden, M.O., 2013. NIST reference fluid thermodynamic and transport properties-REFPROP, Version 9.1, NIST Standard Reference Database 23, National Institute of Standards and Technology, Gaithersburg, MD. <http://www.nist.gov/srd/nist73.cfm>
- Lindley, A.A., Noakes, T. J., 2010. Consideration of hydrofluoroolefins (HFOs) as potential candidate medical propellants. Mexichem Flour Report.
- McLinden, M.O., 1988. Thermodynamic evaluation of refrigerants in the vapour compression cycle using reduced properties. *Int. J. Refrig.* 11, 134-143.
- McLinden, M. O., 1990. Optimum refrigerants for non-ideal cycles: An analysis employing corresponding states. USNC/IIR–Purdue Refrigeration Conference and ASHRAE-Purdue CFC Conference 69-79 (W. Lafayette, IN, July 17-20, 1990).
- McLinden, M. O., Domanski, P. A., Kazakov, A., Heo, J., Brown, J. S., 2012. Possibilities, limits, and tradeoffs for refrigerants in the vapor compression cycle. 2012 ASHRAE/NIST Refrigerants Conference. (Gaithersburg, MD, October 29-30, 2012).
- McLinden, M. O., Kazakov, A. F., Brown, J. S., Domanski, P. A., 2014. A thermodynamic analysis of refrigerants: Possibilities and tradeoffs for Low-GWP refrigerants. *Int. J. Refrig.* 38, 80-92, doi:10.1016/j.ijrefrig.2013.09.032
- McLinden, M. O., Kazakov, A. F., Brown, J. S., Domanski, P. A., 2015 Hitting the bounds of chemistry: Limits and tradeoffs for low-GWP refrigerants. 24th Int. Congress of Refrig. (Yokohama, Japan, August 16-22, 2015).
- McLinden, M. O., Brown, J. S., Kazakov, A. F., Brignoli, R., Domanski, P. A., 2017. Limited options for low-global-warming-potential refrigerants. *Nature Communications*, 8:14476, doi: 10.1038/ncomms14476.
- Middleton, W. J., Sharkley, W. H., 1959. Fluoroacetylene. *J. Am. Chem. Soc.* 81, 803-804.
- Midgley, T., 1937. From the periodic table to production. *Ind. Eng. Chem.* 29, 241-244.
- Muller-Steinhagen, H., Heck K., 1986. A simple pressure drop correlation for two-phase flow in pipes, *Chem. Eng. and Process.*, 20, 297-308.
- Myhre, G. et al., 2013. in *Climate Change 2013: The Physical Science Basis, Fifth Assessment Report of the Intergovernmental Panel on Climate Change.* Cambridge University Press 2013.
- UNEP, 2016. Amendment to the Montreal Protocol on Substances that Deplete the Ozone Layer, Kigali, 15 October 2016. <https://treaties.un.org/doc/Publication/CN/2016/CN.872.2016-Eng.pdf> (accessed January 8, 2017).
- Schuster, P. X., 2009. Biotransformation of trans-1,1,1,3-tetrafluoropropene, 2,3,3,3-tetrafluoropropene and 1,2,3,3,3-pentafluoropropene, Bayerischen Julius-Maximilians-Universität Würzburg.
- Wojtan, L., Ursenbacher T., Thome J.R., 2005a. Investigation of flow boiling in horizontal tubes: Part I - A new diabatic two-phase flow pattern map, *Int. J. Heat and Mass Transfer*, 48, 2955-2969.
- Wojtan, L., Ursenbacher, T., Thome J.R., 2005b. Investigation of flow boiling in horizontal tubes: Part II - Development of a new heat transfer model for stratified-wavy, dryout and mist flow regimes, *Int. J. Heat and Mass Transfer*, 48, 2970-2985.